according to their respective class: curve points in black dots, end points in black filled squares and junctions in black filled circles. Fig. 1*c* shows the skeleton by influence zone of the skeleton branches, *SKIZ*(*S*), shown as thick lines drawn on the skeleton image, allowing decomposition of the sample shape into regions, as shown in Fig. 1*d*. Finally, from the shape decomposition we achieve the boundary segmentation shown in Fig. 1*e*. We are currently working on modelling each token according to perceptual salient attributes and arranging shape tokens for an effective shape indexing.

 8 May 2002
Electronics Letters Online No: 20020724
DOI: 10.1049/el:20020724

C. Di Ruberto (*Department of Mathematics, University of Cagliari, Via Ospedale 72, 09124 Cagliari, Italy*)

E-mail: dirubert@vaxca1.unica.it

References

1 SANTINI, S., and JAIN, R.: 'Similarity measures', *IEEE Trans. Pattern Anal. Mach. Intell.*, 1999, **21**, (9), pp. 871–883
2 DI RUBERTO, C., and DEMPSTER, A.G.: 'Attributed skeleton graphs using mathematical morphology', *Electron. Lett.*, 2001, **37**, (27), pp. 1325–1327
3 PELILLO, M., SIDDIKI, K., and ZUCKER, S.W.: 'Matching hierarchical structures using association graphs', *IEEE Trans. Pattern Anal. Mach. Intell.*, 1999, **21**, (11), pp. 1105–1119
4 SERRATOSA, F., ALQUEZAR, R., and SANFELIU, A.: 'Efficient algorithms for matching attributed graphs and function-described graphs'. Proc. 15th Int. Conf. on Pattern Recognition, Barcelona, Spain, 2000, Vol. 2, pp. 867–872
5 SERRA, J.: 'Image analysis and mathematical morphology', vol. 2 (Academic Press, 1992)
6 SOILLE, P.: 'Morphological image analysis: principles and applications' (Springer, 1999)
7 JANG, B., and CHEN, R.T.: 'Analysis of thinning algorithms using mathematical morphology', *IEEE Trans. Pattern Anal. Mach. Intell.*, 1990, **12**, (6), pp. 541–551
8 REINHARDT, J.M., and HIGGINS, W.E.: 'Efficient morphological shape representation', *IEEE Trans. Image Process.*, 1996, **5**, (1), pp. 89–101

Error concealment technique based on optical flow

Jae-Won Suh and Yo-Sung Ho

A new motion vector recovery algorithm based on optical flow is proposed. Optical flow fields are very similar to the true motion and can be used to recover three-dimensional motion information. Experimental results on test video sequences produced a higher peak signal-to-noise ratio value than that of conventional methods based on the block matching algorithm.

Introduction: The fast growth of digital transmission services has generated a great deal of interest in the digital transmission of video signals over a band-limited channel. The bandwidth constraint necessitates the use of efficient coding schemes to compress the video data, such as H.263 and MPEG-2. If some coded bits are lost or corrupted by channel errors during transmission, an appropriate data recovering process is required to obtain acceptable visual quality. Several methods, including automatic retransmission request (ARQ), forward error correction coding (FEC), and the interleaving technique, have been proposed to solve the above problem. However, ARQ may aggravate the channel congestion and can cause a system to drop more data. FEC usually requires too many additional parity bits for error detection and correction. The interleaving technique may require considerable time delay and modification of a video codec.

An alternative approach is the error concealment technique, which reconstructs the lost data by exploiting spatial and temporal redundancies existing in the video sequences. Therefore, we can avoid channel congestion, time delay, and codec modification problems. For spatial-domain error concealment, we can use various interpolation methods to recover the lost data. Motion vector (MV) recovery is one of the critical issues to conceal the corrupted macroblocks (MBs) in the temporal-domain error concealment technique. A number of MV recovery algorithms based on the block matching algorithm have been developed. In this Letter we propose a new MV recovery algorithm based on optical flow to improve video quality.

Conventional error concealment methods: An estimate for the MV of the lost MB can be obtained by taking the average value of MVs of vertically adjacent MBs (AVG) [1] of the lost MB. In this scheme, if vertically neighbouring MBs have MVs, we can obtain reasonably good reconstruction quality for the lost MB. If only one or none of the vertical neighbours has a valid MV, however, quality of the reconstructed image is not satisfactory.

Other conventional error concealment methods use boundary pixels of the lost MB to estimate the lost MV. The boundary matching algorithm (BMA) [2] uses above, below, and left boundary pixels of the lost MB to recover MV. The decoder motion vector estimation algorithm (DMVE) [3] exploits several boundary pixel lines (two to eight) of the lost MB. While the implementation methods of these algorithms are slightly different, they contain almost the same idea. Furthermore, they have significant limitations that left pixels of the lost MB are not available for the MV estimation. Even if left boundary pixels are used for MV recovery, they already include error concealment mismatch from the second position of the MV estimation.

Determining optical flow: Optical flow is the distribution of apparent velocities of movement of brightness patterns in an image. Optical flow arises from relative motion of objects and the viewer. Consequently, optical flow can be corresponded to the motion. To find optical flow is to minimise the error in the optical flow constraint equation and the measure of departure from smoothness as (1) [4].

$$e^2 = \int\int [(E_x u + E_y v + E_t)^2 + \alpha^2 (u_x^2 + u_y^2 + v_x^2 + v_y^2)] dx\, dy \quad (1)$$

Where u and v are the x and y components of the optical flow, E_x, E_y, and E_t means partial derivatives of image brightness with respect to x, y and t, respectively. The minimisation is to be accomplished by finding suitable values for the optical flow velocity (u, v). Using the calculus of variation and the approximation of Laplacian, (1) can be written as

$$\begin{aligned} (\alpha^2 + E_x^2 + E_y^2)(u - \bar{u}) &= -E_x(E_x \bar{u} + E_y \bar{v} + E_t) \\ (\alpha^2 + E_x^2 + E_y^2)(v - \bar{v}) &= -E_y(E_x \bar{u} + E_y \bar{v} + E_t) \end{aligned} \quad (2)$$

α^2 plays a significant role only for areas where the brightness gradient is small, preventing haphazard adjustments to the estimated flow velocity occasioned by noise in the estimated derivatives. This parameter should be roughly equal to the expected noise in the estimated of $E_x^2 + E_y^2$. Optical flow can be computed by a new set of velocity estimates (u^{n+1}, v^{n+1}) from the estimated derivatives and the average of the previous velocity estimates (u^n, v^n) by

$$\begin{aligned} u^{n+1} &= \bar{u}^n - E_x(E_x \bar{u}^n + E_y \bar{v}^n + E_t)/(\alpha^2 + E_x^2 + E_y^2) \\ v^{n+1} &= \bar{v}^n - E_y(E_x \bar{u}^n + E_y \bar{v}^n + E_t)/(\alpha^2 + E_x^2 + E_y^2) \end{aligned} \quad (3)$$

where n is iteration number, and $\bar{u}$ and $\bar{v}$ are local average of velocity.

Proposed error concealment algorithm: The proposed MV recovery algorithm uses the optical flows of correctly decoded neighbouring data as shown in Fig. 1. First, we obtain optical flows of the optical flow region (OFR) by (3). The computations are based on just two frames, which are the current frame and the previously decoded reference frame. Secondly, we take the average of optical flows within the MV estimate block (MVEB) that come in touch with the lost MB. The average value is used as the MV for the lost MB. In this algorithm, how to define the OFR and the MVEB is very important. If the OFR is increased, the computation time is increased. The MVEB is closely related to the accuracy of estimated MV for the lost MB.

Simulation results: To evaluate the performance of the error concealment algorithms, we performed computer simulations on test video sequences: FOOTBALL, BICYCLE, and BALLET. They have the 4:2:0 format of 720 × 480 pixels. These are encoded using the pattern of IBBPBBPBBPBB at 30 frames/s (NTSC). We consider MPEG-2

TS packet system for considering noisy channels. We assume that the first P-frame has lost one TS packet. Performance comparison has been earned out on the original and four algorithms: AVG [1], BMA [2] which has [−25, 25] search range and 1 extension width, DMVE [3] which has [−25, 25] search range and 2 extension width, and the proposed optical flow algorithm (OFA). The width of the OFR is 32 pixels and the size of the MVEB is the same as that of an MB. Therefore, we need 32 iterations to obtain optical flow of the OFR.

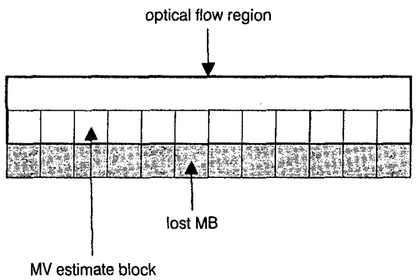

Fig. 1 *Error concealment algorithm using optical flow*

Table 1 summarises the peak signal-to-noise ratio (PSNR) for the three test video sequences. The Table shows that the proposed OFA produces the best PSNR of all the methods. As shown in Fig. 2, we can achieve better subjective video quality using the proposed OFA in the BALLET and BICYCLE video sequences.

Table 1: PSNR comparison of concealed P-frame

Conceal methods	PSNR [dB]		
	FOOTBALL	BALLET	BICYCLE
Original	32.58	29.12	26.57
AVG	30.62	28.41	25.15
BMA	31.24	28.53	23.37
DMVE	31.23	28.52	23.30
OFA	31.76	28.87	25.21

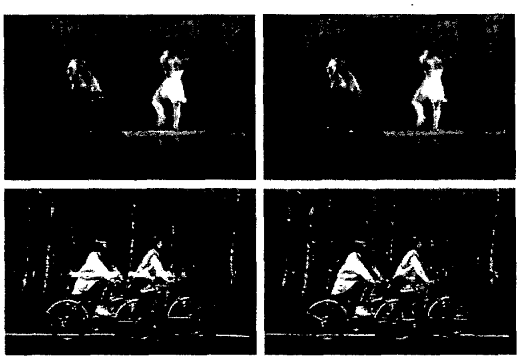

a b

Fig. 2 *Subjective quality comparison of BALLET and BICYCLE*
a Block matching algorithm
b Proposed optical flow algorithm

Conclusion: We have described various error concealment algorithms for the MPEG-2 video transmission system. The simulation results indicate that the proposed OFA produces a higher PSNR value when compared to conventional methods. While conventional methods have a big computation burden due to motion estimation in the decoder, OFA requires several iterations. These results lead us to the conclusion that the proposed OFA is one of the best solutions for error concealment.

26 February 2002
Electronics Letters Online No: 20020733
DOI: 10.1049/el:20020733

Jae-Won Suh and Yo-Sung Ho (*Department of Information and Communications, Kwangju Institute of Science and Technology, 1 Oryong-Dong Puk-Gu, Kwanju 500-712, Korea*)

References

1 SUN, H., CHALLAPALI, K., and ZDEPSKI, J.: 'Error concealment in digital simulcast AD-HDTV decoder', *IEEE Trans. Consum. Electron.*, 1992, **38**, pp. 108–116
2 LAM, W.M., REIBMAN, A.R., and LIU, B.: 'Recovery of lost or erroneously received motion vectors'. Proc. ICASSP, Minneapolis, Minnesota, USA, April 1993, Vol. 5, pp. 417–420
3 ZHANG, J., ARNOLD, J.F., and FRATER, M.R.: 'A cell-loss concealment technique for MPEG-2 coded video', *IEEE Trans. Circuits Syst. Video Technol.*, 2000, **10**, pp. 659–665
4 HORN, B.K.P., and SCHUNCK, B.G.: 'Determining optical flow', *Artif. Intell.*, 1981, **17**, pp. 185–203

Multiwavelet packet transforms with application to texture segmentation

Jing-Wein Wang

The authors have formulated the segmentation problem upon a textured image as an optimisation problem and adapted evolutionary algorithms for the selection in wavelet feature space. The purpose is to demonstrate the efficiency of Geronimo-Hardin-Massopust (GHM) multiwavelets in texture discrimination with respect to D4 scalar wavelets.

Introduction: Multiwavelets have increasingly attracted much theoretical attention and provided a good indication of a potential impact on signal processing [1]. In this Letter, a novel texture segmentation scheme is proposed both to extend the experimentation made in [1] and to test the effectiveness of the Geronimo-Hardin-Massopust (GHM) discrete multiwavelet transform (DMWT) with respect to the D4 scalar wavelet [2]. A problem in genetic wavelet texture analysis is that the chromosomes interact only with the fitness function, but not with each other. This method precludes the evolution of collective solutions to problems, which can be very powerful. We further present an evolutionary framework for feature selection in which successive generations adaptively develop behaviour in accordance with their natural needs.

Feature extraction: Recently Wang *et al.* [3] introduced the extrema number as a particular feature of coarseness, being very useful as a distinctive measure for the works of texture classification. Features that perform better in a classification environment should have a stronger potential to perform better in an image segmentation role. This interpretation prompted us to use the extrema density of wavelet coefficients as a measure of coarseness of the texture. Coarseness at a pixel is considered as the extrema density in a square window $N^2 (N \in Z)$ around the corresponding wavelet coefficients. Thus, the wavelet extrema density (WED) measure, the number of extrema per unit area in row and column scans for the wavelet coefficients of two-dimensional (2D) signal $f(Wf)$, of the pixel p is defined by

$$\mathrm{WED}_p = \frac{1}{N^2} \sum_{i=1}^{N} \sum_{j=1}^{N} W_e f(i,j)$$

$$W_e f = \{\mathrm{Max}_r Wf \cap \mathrm{Max}_c Wf, \mathrm{Max}_r Wf \cap \mathrm{Min}_c Wf \\ \mathrm{Min}_r Wf \cap \mathrm{Max}_c Wf, \mathrm{Min}_r Wf \cap \mathrm{Min}_c Wf\} \qquad (1)$$

The operators Max_r and Min_r denote the co-ordinates of local row maximum and row minimum, respectively. Local column maximum Max_c and column minimum Min_c are similarly defined. A pixel is a local extremum if it is both a local row extremum (maximum or minimum) and a local column extremum. Coarseness of an image is not an absolute measure, but depends on the level at which the image processed. The low resolution subbands make a textured surface seem smoother, while the subbands bring forward the rough structure of the surface at high resolution. Moreover, the larger the size of the window the more reliable were the texture features found; however, the less accurate the boundaries between feature clusters become. This leads to a trade-off between choosing good region segmentation or good boundaries between regions.